

## Significance of the depth-related transition montmorillonite-beidellite in the Bouillante geothermal field (Guadeloupe, Lesser Antilles)

DELPHINE GUISSÉAU,<sup>1</sup> PATRICIA PATRIER MAS,<sup>1,\*</sup> DANIEL BEAUFORT,<sup>1</sup> JEAN PIERRE GIRARD,<sup>2</sup> ATSUYUKI INOUE,<sup>3</sup> BERNARD SANJUAN,<sup>2</sup> SABINE PETIT,<sup>1</sup> ARNAUD LENS,<sup>1,†</sup> AND ALBERT GENTER<sup>2</sup>

<sup>1</sup>UMR 6532 CNRS, HydrASA, University of Poitiers, 40 Avenue du Recteur Pineau, 86022 Poitiers Cedex, France

<sup>2</sup>BRGM, 40 Avenue Claude Guillemin, BP 6009, 45060 Orléans Cedex, France

<sup>3</sup>Department of Earth Sciences, Chiba University, Chiba 263-8522, Japan

### ABSTRACT

The crystal structure and crystal chemistry of dioctahedral smectites in high-enthalpy geothermal systems were investigated through samples collected in two wells drilled in the Bouillante geothermal area to understand the factors that control their vertical variation. Smectites were examined by optical and scanning electron microscopy, electron microprobe analysis, X-ray diffraction (XRD), Fourier transform infrared spectrometry (FTIR), and oxygen-isotope analysis. Smectites predominate within the upper part of the drill holes (up to 260 m depth; temperature range: 67–163 °C). The XRD, FTIR, and chemical microanalyses clearly demonstrate a transition from montmorillonite to beidellite with increasing depth and temperature that proceeded through interstratification of beidellite-like and montmorillonite-like layers. Montmorillonite predominates at temperatures below 100 °C, whereas beidellite predominates between 110 and 163 °C. However, this transition is not explained by a thermally controlled beidellitization process but appears to be related to hydrothermal fluids from which these smectites precipitated. The  $\delta^{18}\text{O}$  values of the fluids that equilibrated with smectites (–3.3 to 0.4‰) indicate that beidellitic smectite precipitated from the hot geothermal fluid associated with minor amounts of residual solutions resulting from local boiling. In the same way, montmorillonitic smectite precipitated from reacting solutions whose origin lies in the phreatic water table ( $\pm$ seawater contribution) associated with minor amounts of liquids resulting from the condensation of vapors escaped from the boiling zones. The mixing rate of geothermal fluid with meteoric waters exerted a major influence on the montmorillonite vs. beidellite ratio of the smectite material as underlined by the irregular depth-related smectite transition.

**Keywords:** Beidellite, montmorillonite, crystal chemistry, crystal-structure, oxygen isotope, high enthalpy geothermal field, Bouillante, Guadeloupe

### INTRODUCTION

Dioctahedral smectites are particularly abundant in the outermost alteration zone of high-temperature (250–260 °C) geothermal fields (Bargar and Beeson 1981; Cathelineau et al. 1985; Cole and Ravinsky 1984; Flexser 1991; Inoue et al. 1999; Reyes 1990; Seki 2000, among others). These clay minerals are classic products of weathering under surface conditions and/or of hydrothermal alteration process (Güven 1988; Inoue 1995; Righi and Meunier 1995; Velde 1985). In active hydrothermal systems related to felsic to intermediate volcanic complexes, dioctahedral smectites constitute index minerals of the argillic alteration zone (Browne and Ellis 1970; Hulen and Nielson 1984; Inoue 1995; Lowell and Guilbert 1970) in which they are considered a product of the alteration of rocks by near-neutral solutions at temperatures ranging from less than 50 to about 170

°C (Bargar and Beeson 1981; Flexser 1991; Inoue 1995; Reyes 1990; Wohletz and Heiken 1992, among others). However, even if the dioctahedral smectites could be a potential guide for hidden high-temperature reservoirs zones, they have been poorly studied and, in the literature, they are generally reported under the generic term of montmorillonite.

A few studies have pointed out different types of dioctahedral smectites (montmorillonite, beidellite, or nontronite) in the outermost alteration halo of high-enthalpy geothermal fields (Beaufort et al. 1996; Inoue et al. 2004; Yang et al. 2001). However, until today, no systematic investigations have been performed on the crystal chemistry of the dioctahedral smectites in such geothermal systems, and little is known about the parameters that control the existing variations at the field scale.

The absence of reliable data on hydrothermal smectites can be attributed to several factors. First, most attention has been paid to clay minerals that crystallized in the reservoirs at higher temperature, and, more particularly, to the mechanism of the late illitization stage (Battaglia 2004; Drits et al. 1996; Harvey and Browne 1991; Inoue et al. 1988; Inoue and Kitagawa 1994; Ji

\* E-mail: patricia.patrier@univ-poitiers.fr

† Present address: Arcelor Research, Voie Romaine, 57283 Maizières-les Metz, France.

and Browne 2000). Second, close to the surface, the outermost hydrothermal halos are frequently obliterated by clay minerals formed under weathering conditions (generally smectite or minerals of the kaolin family).

The geothermal field of Bouillante is a good candidate for a detailed investigation of the spatial variation of the properties of dioctahedral smectites in hydrothermal systems. Previous works have demonstrated that both the present and the fossil geothermal activities identified at the surface of the geothermal field have resulted in the crystallization of dioctahedral smectites, easily distinguishable from the weathering clays formed over all the Basse Terre island (kaolinite/smectite mixed-layers and halloysite) (Patrier et al. 2003). In 2001, three directional wells were drilled through the geothermal field of Bouillante. All these drill holes intersect a zoned alteration profile with a smectite-rich outermost zone (250 to 300 m thick) in which rocks are presently altered at temperature ranging from 50 to 175 °C (Mas et al. 2006).

The aim of this study was to investigate the crystal structure and crystal chemistry of the dioctahedral smectites formed at different depths and temperatures within the Bouillante geothermal field to better understand the factors that control their vertical variation (temperature, fluid/rock ratio, fluid and rock chemistry). Special attention was paid to the depth-related montmorillonite to beidellite transition that is controlled on one hand by the high geothermal gradient existing at present and, on the other hand, by the chemical nature of the solutions involved in the mineralogical reactions.

## GEOLOGICAL SETTING

The geothermal field of Bouillante is located on the western coast of the Basse-Terre Island, Guadeloupe, which belongs to the Lesser Antilles active island arc (Fig. 1). According to Traineau et al. (1997), the geothermal activity of the area is associated with fissure-type volcanic activity that is related to a major regional tectonic lineament oriented NNW-SSE (the Basse Terre-Montserrat fault system). The recent volcanic activity is expressed by the “Bouillante Volcanic Chain” (<1 My) that generated several eruptive centers (Traineau et al. 1997). The geothermal area of Bouillante is located at the point of convergence between the NNW-SSE striking faults system, mainly recognized offshore, and a swarm of ~east-west striking normal faults observed on the island, which display a geometry similar to that observed farther east between Grande Terre and Marie Galante (Feuillet et al. 2002).

The bay of Bouillante presents numerous surface hydrothermal features such as hot springs, mud pools, steaming grounds, and fumaroles (Sanjuan et al. 2000). The mineral assemblage associated with this surficial hydrothermal activity consists mainly of beidellitic smectite (i.e., aluminous smectite in which the octahedral charge is lower than the tetrahedral one) + zeolites + calcite + quartz (Patrier et al. 2003).

In 2001, three directional wells (BO5, BO6, and BO7) were drilled that allowed the collection of cuttings of the altered rocks up to 800–1000 m (drilling depths). These drill holes intersected intercalations of submarine, volcanoclastic formations (tuffs, hyaloclastites, scarce lava flows), and sub-aerial formations (andesitic lava flows, pyroclastites, lahars) related to the volca-

nism of the Axial Chain (–1.5–0.6 Ma) (Traineau et al. 1997). Exploration data indicated a high thermal gradient at a shallow depth (with a temperature close to 200 °C at a depth of 350 m) and occurrences of fluids with maximum temperature of 250 to 260 °C close to the intersection with two major faulted horizons at depth near 500–600 and 900 m, respectively. In a previous study based on alteration petrography and mineralogy, Mas et al. (2006) described the deep extension of the hydrothermal system of Bouillante as being composed of three distinctive zones with increasing depth and temperature (Fig. 2): (1) a shallow alteration zone in which dioctahedral smectites largely predominate (at depths and temperatures ranging from 0 to 300 m and from 50 to 175 °C, respectively); (2) an intermediate alteration zone in which illite and I/S mixed layers (I > 85%) are associated with variable amounts of chlorite (at depths and temperatures ranging from 300 to 700 m and from 180 to 250 °C, respectively); and (3) a deep alteration zone in which chlorite largely predominates over illite (from 700 to the bottom of the drill holes and from 250–260 °C).

Mas et al. (2006) described smectite as the index mineral of the shallow alteration zone in which most of the rock-forming minerals (i.e., plagioclase and pyroxene) have been replaced by a hydrothermal assemblage of smectite + calcite ± hematite and considered this expandable clay mineral as indicator of the so-called argillic facies. These authors also indicated that, in the shallow alteration zone, smectite and calcite are newly formed minerals that obliterated previously formed secondary silicates whose mineralogical properties seem to be depth related: zeolites of the heulandite-clinoptilolite group (0–125 m, 80–100 °C), wairakite, minor pumpellyite and epidote (from 246 m, for  $T > 150$  °C), and disseminated minerals of the chlorite group (corrensite, chlorite) ± early carbonates that previously replaced primary pyroxenes and glass inclusions at depth below 125 m.

Both the chemical and physical characteristics of the geothermal fluids collected in the productive wells are quite similar, suggesting a common origin (Traineau et al. 1997; Sanjuan et al. 2001). The high-temperature geothermal fluids collected in the different wells consist of NaCl water with TDS around 20 g/L and a pH of  $5.3 \pm 0.3$  (see Mas et al. 2006, for the reconstructed chemical and isotopic compositions of the geothermal fluids and associated incondensable gases). These fluids are considered to be a mixture of 58% sea water and 42% fresh water on the base of their Cl and Br concentrations and their  $\delta D$  values. In this case, as no  $^{18}O$  enrichment due to interaction processes with silicate and carbonate minerals is observed,  $\delta^{18}O$  values of the geothermal fluids can be also used to estimate the proportions of this mixing. All these values were previously corrected using the steam-liquid proportions at separation temperature and pressure. According to Sanjuan et al. (2001), the mean  $\delta^{18}O$  value for the geothermal fluids was estimated to be close to  $-1.1 \pm 0.2\text{‰}$ . A mean value of about  $-3.0 \pm 0.5\text{‰}$  can be selected for the surface meteoric waters present in the Bouillante area. From several analytical measurements, a value of  $0.4 \pm 0.2\text{‰}$  was selected for the local seawater of the Bouillante area. This value, slightly higher than 0‰ value for the standard mean ocean water (SMOW), is characteristic of an enclosed sea such as the Caribbean Sea. According to their chemical and isotopic compositions, the geothermal fluids have reacted with volcanic rocks (such as

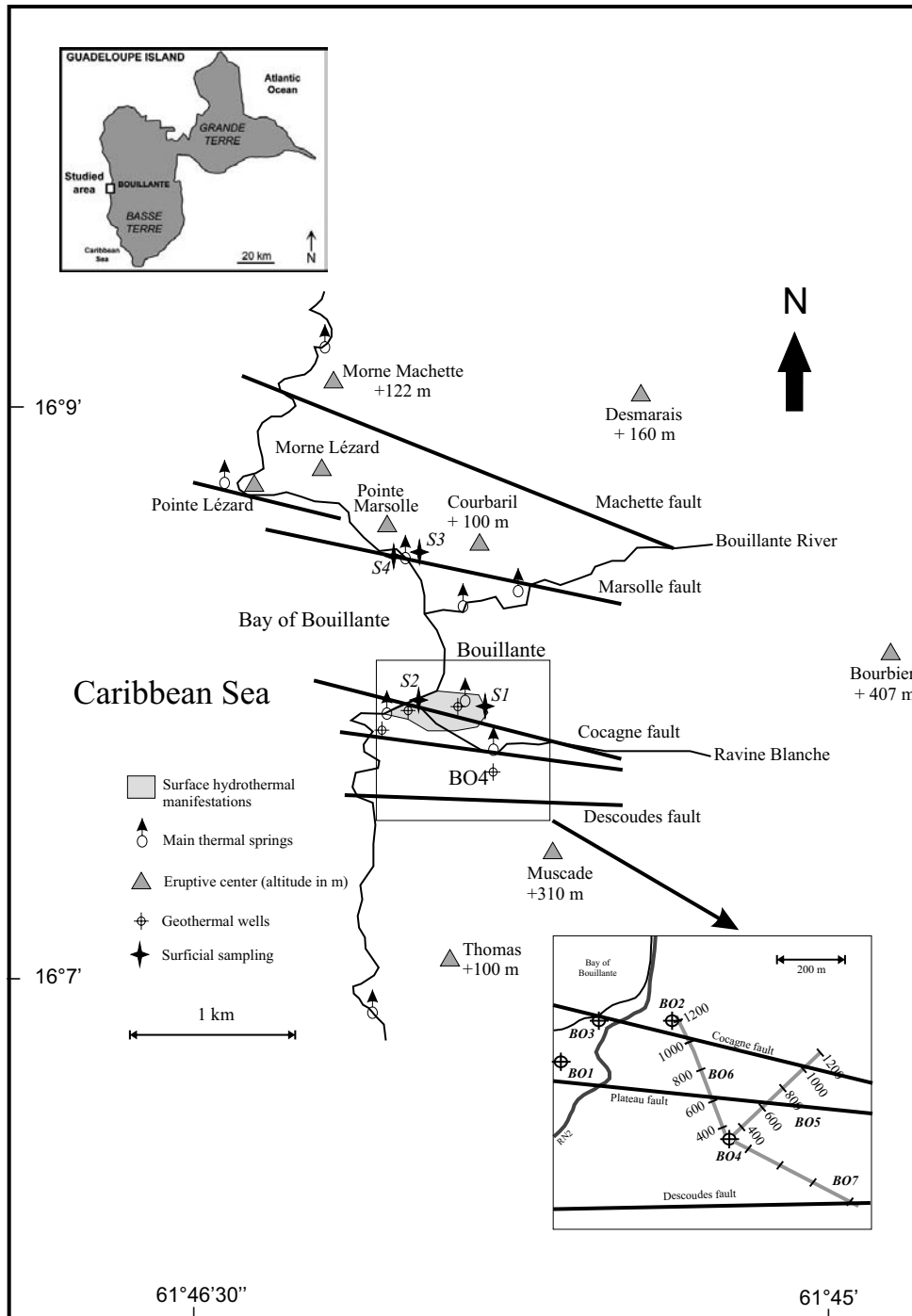


FIGURE 1. Location of the studied area in Guadeloupe Island and schematic map of the Bouillante Bay showing the location of the wells and the main surface hydrothermal features. The bold lines represent the main tectonic faults identified by Traineau et al. (1997). Modified from Mas et al. (2006).

andesites or basalts) and have reached an equilibrium state with a mineralogical assemblage in the reservoir at 250–260 °C. This mineralogical assemblage is described in Sanjuan et al. (2001) and in Mas et al. (2006). The geothermal fluids are enriched in K, Ca, Si, B,  $\text{NH}_4$ ,  $\text{H}_2\text{S}$ , Li, Sr, Ba, Mn, Cs, Rb, As, and trace metal ions. They are depleted in Mg,  $\text{SO}_4$ , and Na relative to

seawater diluted by 42% fresh water. The Mg concentration of the reservoir fluids collected in all the productive wells is <10 mg/L (Traineau et al. 1997). Consequently, it is expected that the geothermal fluids collected at Bouillante have precipitated significant amounts of magnesian clays in the deeper part of the geothermal system of Bouillante (Mas et al. 2006).

SAMPLES AND METHODS

Eighteen samples of altered rocks were collected within the smectite zone of the geothermal field of Bouillante. Their main characteristics are summarized in Table 1. Fourteen samples (cuttings) were collected in the smectite zone intersected by drill holes BO6 and BO7. These samples were collected at relatively regular intervals within the 40–260 m depth range (corresponding to a 70–160 °C temperature range). Four additional samples were selected from among the hundreds of surface samples of the geothermal field previously studied by Patrier et al. (2003). The location of these surficial smectites, selected to complete the oxygen isotope data of the in-hole smectites, is reported in Figure 1. Two of them (S1 and S2) were collected in mud pools or steaming grounds located near the center of the geothermal area of Bouillante. The two others (S3 and S4) were collected in hydrothermal veins (as fracture-sealing material) occurring in parts of the geothermal field where no surficial hydrothermal activity occurs at present (Patrier et al. 2003).

Each sample was gently ground in a mortar or in an automatic shatterbox. The obtained powders were then dispersed in distilled water by ultrasonic vibration to disaggregate the particles. All experiments were carried out on infra 0.2 μm fractions. This size fraction was extracted from the <2 μm stabilized clay suspension by continuous ultracentrifugation (Beckman J2-21, rotor speed = 5000 rpm, flow rate = 150 mL/min). These clay fractions were saturated with 1 N CaCl<sub>2</sub> to obtain homo-ionic particles and to maintain similar expandability measurements between the samples. The obtained Ca-clays were then washed with deionized water until they were chloride free (by AgNO<sub>3</sub> test).

XRD was performed with a Siemens D501 diffractometer (Ni-filtered CuKα<sub>1-2</sub>

radiation, 30 mA, 40 KV) equipped with a Peltier-cooled Si detector, and the diffractograms were recorded by a SOCABIM system for numerical data acquisition. Oriented clay mounts were successively analyzed in the air-dried condition and then after ethylene glycol solvation using a spray. They were prepared by filter peel (pore diameter of 0.08 μm). This method produces mounts that have reasonable crystallite orientation (Bish and Reynolds 1989). Powders of clay separates were randomly oriented using a back-loading method, as recommended by Moore and Reynolds (1997). The XRD data of oriented mounts and randomly oriented powders were acquired between 2.5 and 30 °2θ (CuKα) and between 2.5 and 65 °2θ, respectively, with a step size of 0.025 °2θ and a counting time of 3 s per step. The characteristics of the superimposed XRD reflections (position, intensity and FWHM) were determined by deconvolution of diffractograms using the Decomprx software (Lanson and Besson 1992). The NEWMOD program (Reynolds 1985) was used to simulate XRD patterns and to provide a basis for interpretation of the acquired XRD patterns.

The mean layer charge of the smectites was estimated using a single alkylchain with nC = 12 according to the alkylammonium ion-exchange method presented by Olis et al. (1990). The alkyl ammonium-saturation was realized by two successive washings with alkyl ammonium nC = 12 chloride (1 h at 20 °C; 48 h at 60 °C). The excess of alkylamine and chloride were removed by repeated contact with ethanol (1 h at room temperature, then 24 h at 60 °C, and 3 × 15 mn at room temperature). Depending on the magnitude of the layer charge, the alkylammonium ions may adopt either a monolayer (1.36 nm), either a double layer (1.77 nm) or either a pseudotrilayer (2.17 nm) configuration in the interlayer position.

The layer charge of natural smectites is distributed over tetrahedral and octa-

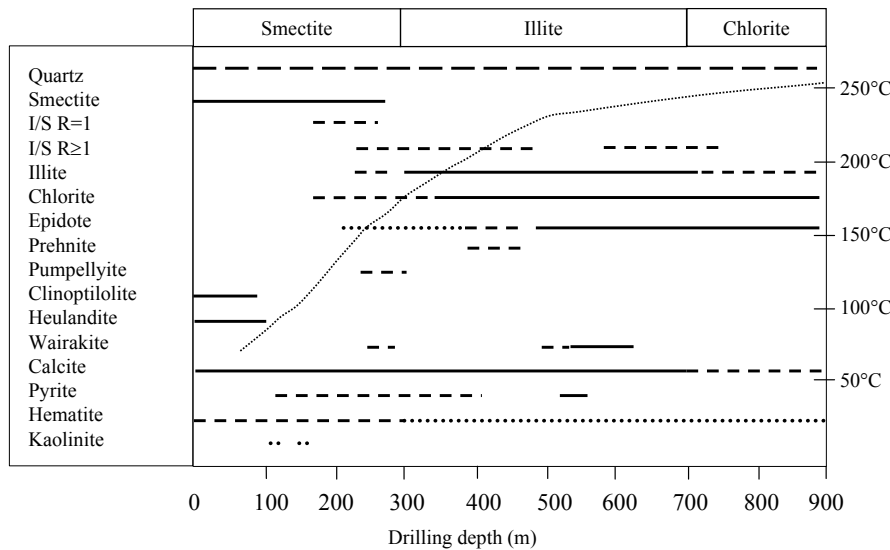


FIGURE 2. Distribution of secondary minerals in well BO6. The smectite, illite, and chlorite zones are defined according to Mas et al. (2006). The curve in the figure is the present day temperature gradient. I/S R = 1: regularly ordered illite/smectite mixed-layers, I/S R ≥ 1: ordered illite/smectite mixed-layers with high illite content (>85%).

TABLE 1. Surficial sampling and drill hole sampling carried out in BO6 and BO7 wells

	Drilling depth (m)	T (°C)	Lithology—BO6/BO7 drill holes
BO7	40	67	Argillized tuff with pyroclastic elements, quartz and calcite
BO7	70	74	Argillized tuff with abundant calcite
BO6	75	76	Lahar and argillized tuff, pyrite and calcite
BO6	110	88	Silicified tuff, calcite
BO7	120	91	Argillized fractured zone with calcite and pyrite
BO6	125	97	Andesitic lava ± altered and argillized
BO6	150	111	Argillized tuff with calcite, silica, anhydrite and chlorite
BO7	155	111	Argillized and fractured zone with kaolinite, silica, calcite and pyrite
BO6	160	115	Fractured zone, argillized tuff/laohar, locally silicified, with abundant calcite
BO7	190	128	Argillized fractured zone with kaolinite, silica, calcite and pyrite
BO7	229	148	Argillized fractured zone with chlorite, calcite and pyrite
BO6	230	150	Fractured zone, tuff/lava ± altered with calcite, silica and pyrite
BO6	236	152	Fractured zone, tuff/lava ± altered with calcite, silica and pyrite
BO6	260	163	Fractured zone, argillized lava with kaolinite, calcite and pyrite
	Surficial samples		Lithology
	S1		Clay material collected in a trench infilled with boiling mud, near BO2
	S2		Strongly altered and argillized rock collected in the steaming ground area
	S3		Cement of a breccia (fossil hydrothermal manifestation)
	S4		Strongly altered hyaloclastite (fossil hydrothermal manifestation)

Note: Lithology was provided by CFG services.

hedral sheets. The octahedral vs. tetrahedral charge distribution in the 2:1 layer of dioctahedral smectites was estimated using XRD on Li-saturated powders heated at 300 °C for 24 h in platinum crucibles to avoid alkali-contamination from the glass slide (Hoffman and Klemen 1950; Greene-Kelly 1953). The octahedral charge is neutralized after this treatment and the tetrahedral charge remains. Therefore, all of the remaining layer charge after the Greene-Kelly test is in the tetrahedral sheets and, according to Calvet and Prost (1971), such smectite remains fully expandable if its tetrahedral charge is higher than 0.19/O<sub>10</sub>(OH)<sub>2</sub>. So, after solvation with ethylene glycol, the *d*<sub>001</sub> spacing of Li-saturated dioctahedral Al-smectites with a predominant octahedral charge (montmorillonite-like character) is collapsed to 9.7 Å, whereas the *d*<sub>001</sub> spacing of those with a predominant tetrahedral charge (beidellite-like character) expands around 17 Å (MacEwan and Wilson 1980). Details on the method used for the Li saturation of smectites can be found in Malfroy et al. (2003).

The CEC was measured using the method described by Righi et al. (1993). Smectite samples were saturated with Mg<sup>2+</sup> and the excess Mg salt (MgCl<sub>2</sub>) was carefully washed with ethanol. Magnesium was then replaced by NH<sub>4</sub><sup>+</sup> and analyzed by atomic absorption spectroscopy. The NH<sub>4</sub><sup>+</sup>-saturated smectites were then washed until they were free of NH<sub>4</sub><sup>+</sup> salts (no reaction with Nessler's reagent) before to be analyzed by FTIR spectroscopy.

Fourier Transform Infrared spectra were recorded with a resolution of 4 cm<sup>-1</sup> in transmission mode in the range 4000–400 cm<sup>-1</sup>, with a NICOLET 510 FTIR spectrometer which was continuously purged with dry air. Spectra were obtained from pressed powder pellets (under 12 tons per cm<sup>2</sup>) prepared with 2 mg of clay and 300 mg of KBr and heated to 110 °C overnight. The measurement of the absorption bands integrated intensity was made using the OMNIC software. The charge distribution of smectite was estimated from FTIR spectra of NH<sub>4</sub><sup>+</sup> and Li-NH<sub>4</sub><sup>+</sup> saturated clays according to the procedure of Petit et al. (1998) which is based on the measurement of the surface variation of the ν<sub>4</sub>NH<sub>4</sub><sup>+</sup> band before and after Li saturation.

The chemical microanalyses of smectites were performed on carbon coated thin sections using a JEOL 5600LV scanning electron microscope [EDS, Si(Li) semi-conductor] with an associated Oxford INCA system. Analytical conditions were 15 kV, 0.65 nA, and 60 s counting time. This system was calibrated using standard minerals (albite, diopside, orthoclase, spessartite, and forsterite) and titanium metal. Corrections were made with an XPP matrix correction (OXFORD INCA system) and the reproducibility is ±1.5%.

Microprobe analyses were also carried out using a CAMECA SX50 electron microprobe equipped with 4 wavelength-dispersive spectrometers (University Pierre et Marie Curie, Paris VI). Analytical conditions were 15 kV, 4 nA, 10 s counting time per element, and 4 μm spot size. The system was calibrated by standard minerals (synthetic oxide or natural standards). Matrix corrections were made with the CAMECA PAP program, and the reproducibility of standard analyses was close to 1% for all elements except Na (1.5%).

Oxygen isotopes analyses were conducted in the stable isotope laboratory of BRGM (Analysis and Mineral Characterization Department). The δ<sup>18</sup>O of smectites was determined by conventional fluorination (Clayton and Mayeda 1963) according to the procedure outlined in Girard et al. (1997). Analysis was performed on 1 to 2 mg of smectite powder. The δ<sup>18</sup>O of calcites were determined on 100–200 mg of bulk rock powders by acidic treatment (100% H<sub>3</sub>PO<sub>4</sub>, 25 °C, 4 h) according to the method outlined by McCrea (1950). Isotopic ratios were measured on a Finnigan MAT252 mass spectrometer. The analytical uncertainty of the δ<sup>18</sup>O values, calculated from repeated analysis of the selected material and laboratory standards, is ±0.4 per mil. These δ<sup>18</sup>O values  $\{[(R_{\text{sample}}/R_{\text{standard}}) - 1] \times 1000 \text{ where } R = {}^{18}\text{O}/{}^{16}\text{O}\}$  are reported relative to the SMOW standard. The δ<sup>18</sup>O values of fluids equilibrated with smectites and calcite were evaluated using the oxygen isotope fractionation between minerals and water proposed by Sheppard and Gilg (1996) and Friedman and O'Neil (1977, following O'Neil et al. 1969), respectively, as a function of temperature:

$$1000 \ln \alpha_{\text{smectite-water}} = 2.55 \times 10^6 \times T^{-2} - 4.05 \quad (1)$$

$$\delta^{18}\text{O}_{\text{calcite}} - \delta^{18}\text{O}_{\text{water}} = 2.78 \times 10^6 \times T^{-2} - 2.89 \quad (2)$$

where *T* is the temperature in Kelvin.

According to Sheppard and Gilg (1996), the smectite-water fractionation factor is applicable for both beidellite and montmorillonite since data from the literature do not show significant variations of oxygen isotope fractionation vs. smectite chemistry.

## RESULTS

### XRD and FTIR characteristics of the smectitic material

XRD patterns of the <0.2 μm fraction of the altered rocks collected at the surface and within the shallow alteration zone of the geothermal field of Bouillante are typical of a clay material composed of 100% smectite layers with a very low saddle/001 peak ratio. Everywhere in the geothermal field, smectite is characterized by a two water layer hydration state at air-dried condition (*d*<sub>001</sub> reflection at 15 Å) and by rational *d*<sub>001</sub>, *d*<sub>002</sub>, and *d*<sub>003</sub> reflections at 17, 8.45, and 5.65 Å, respectively, after ethylene glycol saturation (Fig. 3). Traces of regularly ordered illite/smectite mixed-layers (*R* = 1 type), characterized by weak and broad superstructure and rational reflections near 27.3 and 13.5 Å after ethylene glycol saturation, have been suspected in a few samples collected at depths below 150 m.

XRD patterns of random powder mounts of the <0.2 μm fractions of each sample confirm the dioctahedral and aluminous character of all the smectite samples, with (060,330) reflections close to 1.492 Å. XRD patterns of random powder mounts also indicate that, in most of the samples, the <0.2 μm fraction is

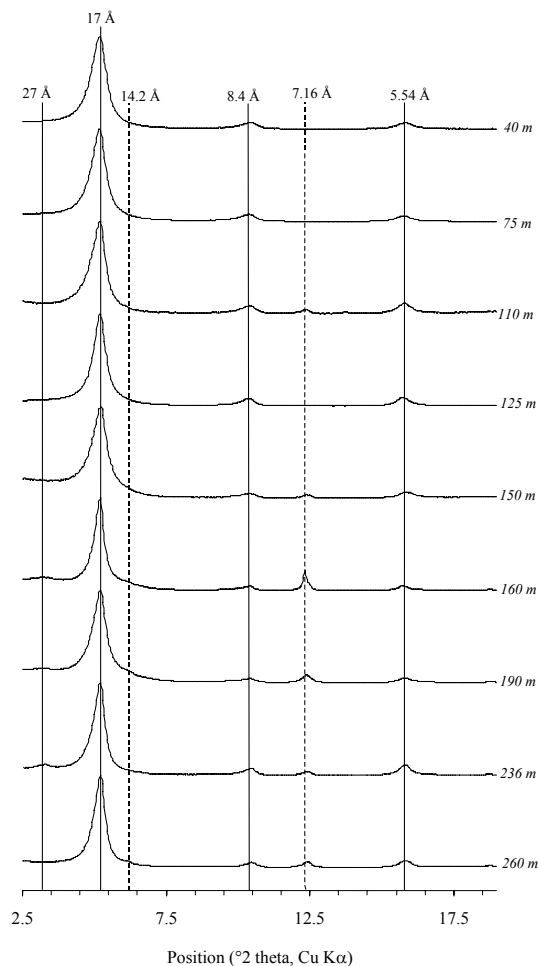


FIGURE 3. Representative XRD patterns of the Ca-saturated smectitic material after ethylene-glycol treatment.

almost monomineralic. Only very small amounts of mineral impurities have been identified in the smectitic material. This is confirmed by the CEC values (included between 63 and 107 meq/100 g) of most of the Ca-saturated samples, which are close to those classically inferred for pure smectites (i.e., 95–120 meq/100 g, Velde 1986). The impurities consist of one or more of the following minerals: calcite, quartz, chlorite, kaolinite, heulandite-clinoptilolite, and plagioclase.

XRD patterns of the borehole samples reveal a depth-related variation that consists in the slight sharpening of the 001 peak of the smectite, suggesting a slight increase in the size of the coherent scattering domain along the *c*-axis direction of the crystallites with increasing depth and temperature (Fig. 3). Such variation of the peak profiles can be illustrated by measuring the full-width at half-maximum intensity (FWHM) of the 001 peak of the Ca-saturated smectite after ethylene glycol-saturation. The FWHM value diminishes from 0.62 to 0.45 °2 $\theta$  (CuK $\alpha$ ) with increasing depth and temperature (Table 2). However such a vertical variation of the FWHM is not perfectly regular with, in particular, an unusually high value (0.70 °2 $\theta$ ) recorded for the smectite collected at a depth of 160 m.

Analyzed in the stretching vibration region, the infrared spectra of all the smectite samples display an Al-OH-Al band near 3630–3660 cm<sup>-1</sup> that is characteristic of dioctahedral aluminous smectites (Farmer 1974). The characteristics of the FTIR spectra in both the stretching and bending vibration regions illustrate a depth-related transition from montmorillonite to beidellite in the smectitic material of the geothermal field of Bouillante (Fig. 4).

Such a vertical transition is illustrated by a shift of the maximum of the Al-OH-Al band from 3630 to 3660 cm<sup>-1</sup> with increasing depth. The band near 3630 cm<sup>-1</sup> would correspond to montmorillonite, whereas the band near 3660 cm<sup>-1</sup> is characteristic of beidellite (Petit, unpublished data). In the surface samples, the Al-OH-Al band exhibits a broad shoulder around 3600 cm<sup>-1</sup> that is attributed to minor  $\nu$ Fe-Al-OH and/or  $\nu$ Mg-Al-OH vibration bands. The relative intensity of this shoulder decreases with increasing depth and is not perceptible below 110 m.

Three index absorption bands can be observed in the bending vibration region, at 914, 840, and 875–880 cm<sup>-1</sup>, respectively. The first one is identified for all the samples and is interpreted as the  $\delta$ Al-OH-Al vibration in smectites. In all the smectite samples collected below 120 m, the profile of this absorption band is modified by the occurrence of a shoulder toward 930–940 cm<sup>-1</sup>. Such behavior could be related to the crystal chemistry of the dioctahedral smectite.  $\delta$ Al-OH-Al bands at higher wavenumbers would correspond to species with predominant tetrahedral charge (e.g., beidellite), whereas  $\delta$ Al-OH-Al bands near 920 cm<sup>-1</sup> would correspond to species with predominant octahedral charge (e.g., montmorillonite). The relative intensity of these bands (at 914 and 940 cm<sup>-1</sup>) evolves in the same way as the associated 3630 and 3660 cm<sup>-1</sup> bands, respectively. The two other index bands have been observed only in smectite from the upper part of the geothermal field (at depths between 40 and 120 m). The band at

840 cm<sup>-1</sup> is characteristic of  $\delta$ Al-OH-Mg vibrations in smectites whereas the band at 875–880 cm<sup>-1</sup> is characteristic of  $\delta$ Fe-OH-Al vibrations (Russel and Fraser 1994).

### Mean layer charge and charge heterogeneity

XRD patterns of smectites saturated with dodecylalkyl ammonium are similar, with a maximum intensity of the 001 reflection that corresponds to a *d*-spacing between 17 and 18 Å (Fig. 5). Using the equation of Olis et al. (1990), such a *d*-spacing is typical of low-charge smectites with a layer charge ranging from 0.35 to 0.38 per half formula unit. However, the change in the 001 peak shape observed in Figure 5 indicates slight variations in layer charge heterogeneity.

Use of XRD profile decomposition allowed a more accurate characterization of the coexisting domains of smectite having distinct layer charge and their respective evolution with increasing depth or temperature (Fig. 6 and Table 3). The peak profiles of all the smectites formed between a depth of 40 and 230 m have been successfully fitted by the sum of three gaussian curves: (1) a major component around 17.2–17.9 Å (layer charge = 0.35–0.37) and two minor components; (2) one around 15.2–16.8 Å (estimated layer charge = 0.29–0.34); and (3) between 18.3 and 20.4 Å (estimated layer charge = 0.40–0.57). It should be noted that the deeper smectites present a quite homogeneous layer charge distribution. Indeed, the 001 peak profile has been fitted by the sum of only two gaussian curves at 17.88 and 18.35 Å (layer charge = 0.37 and 0.39, respectively) at 236 m and by only one gaussian curve at 17.64 Å (layer charge = 0.37) at 260 m.

In summary, the smectites of the geothermal field of Bouil-

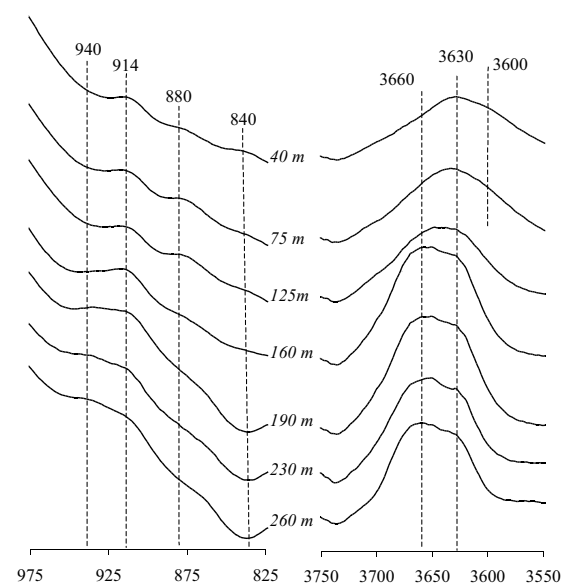
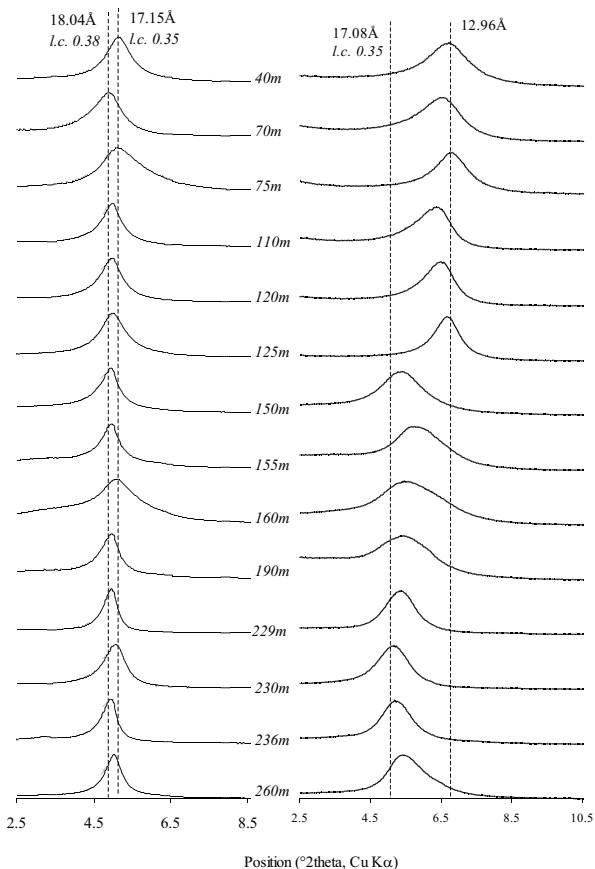


FIGURE 4. Representative FTIR spectra of the Ca-saturated smectitic material in the stretching and bending vibration regions.

TABLE 2. Full width at half-maximum intensity of the (001) reflection of smectite (in °2 $\theta$ , CuK $\alpha$ )

Samples	40	70	75	110	120	125	150	155	160	190	229	230	236	260
FWHM (°2 $\theta$ )	0.62	0.72	0.57	0.57	0.53	0.63	0.58	0.58	0.70	0.49	0.41	0.52	0.46	0.45



**FIGURE 5.** XRD patterns of smectite saturated with dodecylalkyl ammonium. Ca-alkylammonium saturated-sample (on the left part) and Li-alkylammonium saturated sample (on the right part) preparations. l.c. = smectite layer charge per half formula unit (deduced from the equation of Olis et al. 1990).

lante are predominantly low-charge smectites whose layer charge heterogeneity tends to decrease with increasing depth and temperature. As already noted for the variation of peak FWHM, the vertical variation of layer charge distribution in smectite is not regular with, in particular, an unusually heterogeneous layer charge distribution at the depth of 160 m.

#### Variation of charge location

Most of the diffractograms obtained after the Greene-Kelly test display a  $d_{001}$  reflection close to 17 Å and a non-rational  $d_{002}$  reflection at a position between 8.55 and 9.05 Å. Such  $d_{002}$  spacings range between the theoretical  $d_{002}$  reflection of the beidellite and the  $d_{001}$  reflection of the montmorillonite end-members located at 8.5 and 9.7 Å, respectively (Fig. 7). XRD profile decomposition of the experimental pattern and simulation of the resultant gaussian curves using Newmod software (Reynolds 1985) have been used to determine the different components composing the complex peaks of smectite located between 8.5 and 9.7 Å (Fig. 8). XRD peak profile of the complex  $d_{002}$  reflection of the smectitic material collected at the surface and at very shallow depths (<75 m) were fitted by a sum of two phases: (1) discrete montmorillonite, and (2) montmorillonite-beidellite

**TABLE 3.**  $d_{001}$  spacings of elemental curves of XRD patterns of smectite saturated with dodecylalkylammonium "C<sub>12</sub> AA" (deduced from diffractogram decomposition) and smectite layer charge per half formula unit, in italics, deduced from the equation of Olis et al. (1990)

Samples	$d_{001}$ spacings of C <sub>12</sub> AA smectites (in Å) and layer charges (per half formula unit)		
BO7-40	19.62 <i>0.54</i>	<b>17.22</b> <b>0.35</b>	15.89 <i>0.31</i>
BO7-70	20.40 <i>0.58</i>	<b>17.94</b> <b>0.37</b>	15.75 <i>0.31</i>
BO6-75	17.61 <i>0.37</i>	<b>17.24</b> <b>0.35</b>	15.61 <i>0.30</i>
BO6-110	19.65 <i>0.54</i>	<b>17.79</b> <b>0.37</b>	16.18 <i>0.32</i>
BO7-120	19.73 <i>0.54</i>	<b>17.79</b> <b>0.37</b>	15.87 <i>0.31</i>
BO6-125	19.42 <i>0.53</i>	<b>17.71</b> <b>0.37</b>	16.39 <i>0.33</i>
BO6-150	19.36 <i>0.52</i>	<b>17.92</b> <b>0.37</b>	16.59 <i>0.33</i>
BO7-155	19.48 <i>0.53</i>	<b>17.88</b> <b>0.37</b>	16.58 <i>0.33</i>
BO6-160	20.36 <i>0.57</i>	<b>17.36</b> <b>0.36</b>	15.24 <i>0.29</i>
BO7-190	19.31 <i>0.52</i>	<b>17.77</b> <b>0.37</b>	16.06 <i>0.32</i>
BO6-230	19.19 <i>0.52</i>	<b>17.51</b> <b>0.36</b>	16.79 <i>0.34</i>
BO6-236	18.35 <i>0.39</i>	<b>17.88</b> <b>0.37</b>	
BO6-260		<b>17.64</b> <b>0.37</b>	

Note: Values in bold correspond to the main elemental component.

random mixed layer (60% montmorillonite). The complex  $d_{002}$  reflection of the smectitic material collected deeper in the drill holes was fitted by a sum of two distinctive montmorillonite-beidellite random mixed layers in which the amount of montmorillonite-like layers decreases with increasing depth. The total amount of montmorillonite-like layers contained in the deeper samples is probably lower than indicated in Figure 8. Indeed, it should be noted that the position of complex  $d_{002}$  reflection of the smectitic material analyzed at depths below 200 m is close to that of a beidellite and according to the accuracy of the method, it is not possible to differentiate montmorillonite-beidellite random mixed layers with 5% of montmorillonite from a true beidellite (0% montmorillonite). Besides the heterogeneity in crystal structure of the smectitic material, the above data confirm that the global amount of montmorillonite-like layers strongly decreases with increasing depth and temperature.

The respective percentage of both the variable tetrahedral positive charge and the octahedral charge of the 2:1 layer has been determined by two distinctive methods: (1) measuring the areas of the  $\nu_4$  NH<sub>4</sub><sup>+</sup> band before and then after Li treatment using FTIR spectroscopy (Petit et al. 1998), and (2) determining the difference between the CEC values of the Ca-saturated and the

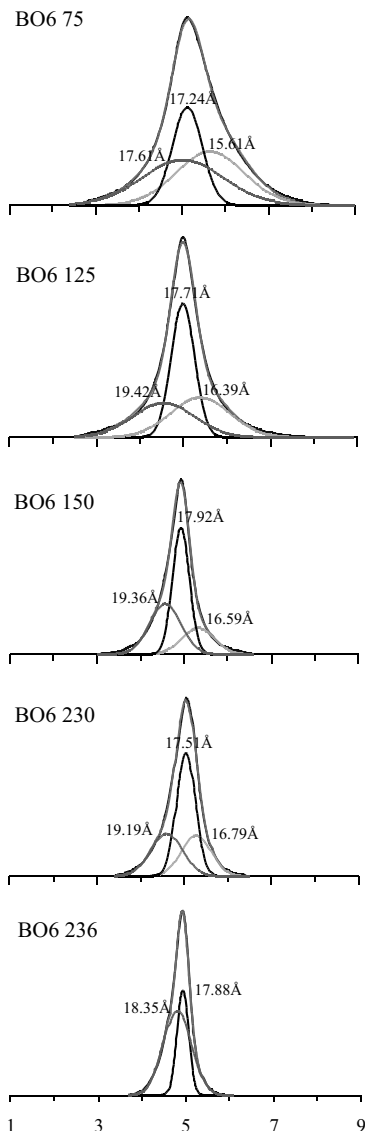


FIGURE 6. Decomposition of representative XRD patterns of smectite (001 reflection) saturated with dodecylalkyl ammonium, using DECOMPXR software. Air-dried state.

TABLE 4. Distribution of smectite layer charges deduced from CEC measurements and FTIR analysis

	CEC		FTIR	
	Tetr. ch. (+ var. ch.)	Oct. ch.	Tetr. ch. (+ var. ch.)	Oct. ch.
BO7-40	23%	77%	22%	78%
BO6-75	25%	75%	36%	64%
BO6-110	78%	22%	72%	28%
BO7-120	–	–	47%	53%
BO6-125	46%	54%	57%	43%
BO6-150	90%	10%	98%	2%
BO7-155	–	–	–	–
BO6-160	82%	18%	98%	2%
BO7-190	–	–	96%	4%
BO7-229	–	–	89%	11%
BO6-230	75%	25%	94%	6%
BO6-236	78%	22%	79%	21%
BO6-260	64%	36%	82%	18%

Note: Tetr. Ch. = tetrahedral charge, var. ch. = variable charge, Oct. ch. = octahedral charge.

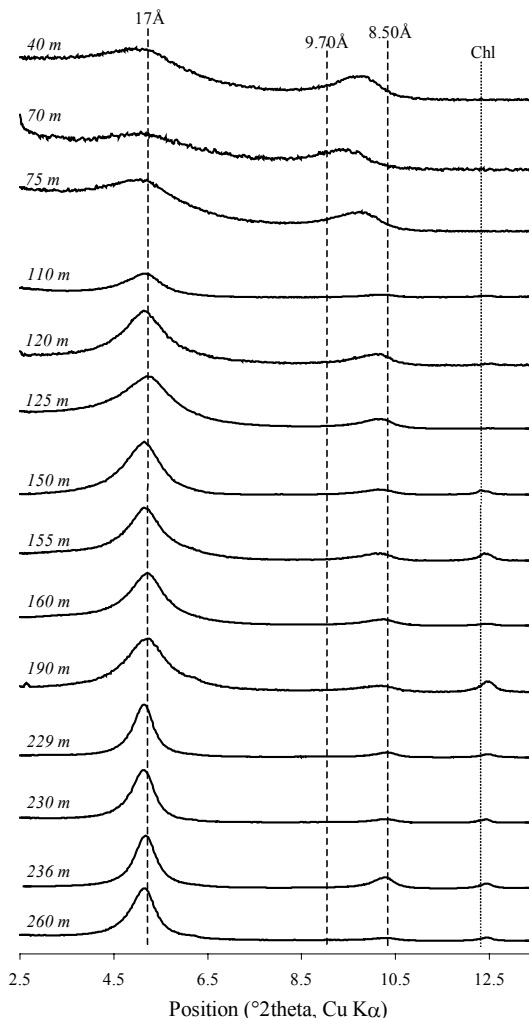


FIGURE 7. XRD patterns of smectites obtained after the Greene-Kelly test (ethylene-glycol-saturated preparations). Chl = chlorite.

Li-saturated samples of smectite. Despite differences that are attributed to problems of accuracy of both methods (Table 4), the results can be summarized as follows. Only 20% of the 2:1 layer charge of the surface smectites is located in tetrahedral sites, and these smectites can be considered montmorillonite. Between 0 and 125 m, the percentage of tetrahedral charge tends to increase up to more than 50%, yielding a smectite with charge properties intermediate between montmorillonite and beidellite. Deeper down, tetrahedrally charged 2:1 layers of smectite strongly predominate (from 79–98% or from 64–90% according to the method used), and the charge distribution in the 2:1 layer of these smectites is near or close to that of ideal beidellite.

**Chemical composition**

Microprobe analyses indicate that the compositional variation of smectite is minimal in each sample, so the average structural formulae presented in Table 5 can be considered as representative of the smectites formed in the different alteration sites of the altered rocks (feldspar replacements, vug infillings, or altered

**TABLE 5.** Structural formula of smectite on the basis of  $O_{10}(OH)_2$ 

Samples Nb analysis	BO7-40 10		BO6-75 8		BO6-110 11		BO7-120 9		BO6-125 17		BO7-155 18	
	av.	st. dev.	av.	st. dev.	av.	st. dev.	av.	st. dev.	av.	st. dev.	av.	st. dev.
Si	3.98	0.02	3.89	0.05	3.71	0.08	3.61	0.01	3.81	0.02	3.69	0.05
Al <sup>IV</sup>	0.02	0.02	0.11	0.05	0.29	0.08	0.39	0.01	0.19	0.02	0.31	0.05
Al <sup>VI</sup>	1.59	0.01	1.33	0.07	1.71	0.06	1.88	0.02	1.64	0.03	1.82	0.04
Fe <sup>3+</sup>	0.00	0.00	0.33	0.06	0.13	0.03	0.09	0.02	0.13	0.02	0.09	0.02
Mg	0.44	0.01	0.33	0.02	0.16	0.05	0.06	0.01	0.25	0.02	0.10	0.03
Ti	0.00	0.00	0.01	0.01	0.00	0.00	0.00	0.00	0.00	0.00	0.01	0.01
Mn	0.00	0.00	0.00	0.00	0.01	0.01	0.00	0.00	0.00	0.00	0.00	0.00
Oct. Oc.	2.04	0.01	2.00	0.02	2.01	0.03	2.02	0.02	2.02	0.01	2.02	0.02
Ca	0.16	0.01	0.12	0.02	0.13	0.06	0.18	0.03	0.16	0.02	0.17	0.02
Na	0.01	0.01	0.04	0.01	0.10	0.07	0.03	0.01	0.01	0.01	0.05	0.01
K	0.02	0.01	0.14	0.03	0.08	0.02	0.09	0.04	0.04	0.01	0.05	0.02
Int. ch	0.35	0.03	0.41	0.02	0.44	0.08	0.48	0.04	0.37	0.03	0.45	0.05
(O) %	94	5	73	11	34	17	19	5	49	7	31	13
(T) %	6	5	27	11	66	17	81	5	51	7	69	13

Notes: Nb analysis = number of analysis, av. = average, st. dev. = standard deviation, Oct. Oc. = octahedral occupancy, Int. ch = interlayer charge, [O] = percentage of octahedral charge, [T] = percentage of tetrahedral charge.

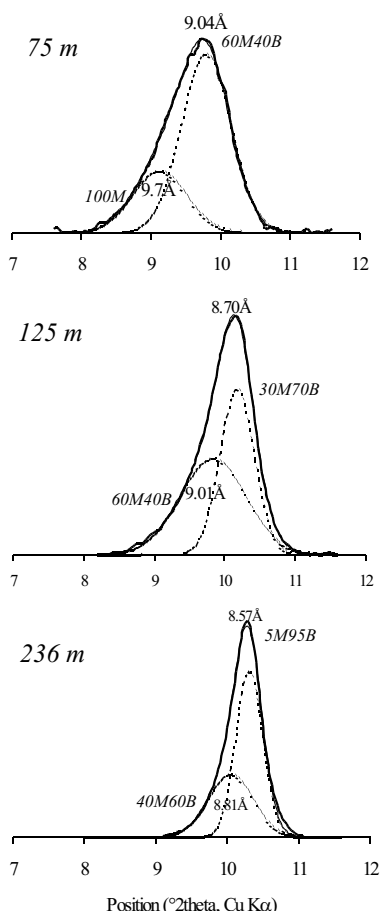


**FIGURE 8.** Decomposition of representative XRD patterns of smectite obtained after the Greene-Kelly test (002 reflection) using DECOMPXR software. Ethylene-glycol-saturated preparations. The amount of beidellite “B” and montmorillonite “M” in the identified mixed-layers are reported in italics.

groundmass). The structural formulae of smectite have been calculated for  $O_{10}(OH)_2$  and total Fe has been arbitrarily considered as  $Fe^{3+}$ .

The fact that the octahedral occupancy is close to 2 confirms the dioctahedral character of the smectite in all the samples and is also indicative of the small amount of mineral impurities at the scale of the analyzed microvolumes. The principal results of the microprobe analyses can be summarized as follows. (1) The interlayer charge of the smectite ranges from 0.35 to 0.52 without any apparent correlation with depth. In all samples, the interlayer charge is mostly satisfied by Ca accompanied by minor but variable amounts of Na and K. And (2) the depth-related chemical variation of smectite mainly consists of a significant decrease in both the Si and Mg contents and conversely an increase in Al content. From the surface to 160 m, Si decreases from 3.98 to 3.49 atoms per formula unit (apfu) and Mg decreases from 0.44 to 0.07 apfu. Deeper down, the Si and Mg contents of smectite remain relatively constant between 3.6–3.5 and 0.05–0.03 apfu, respectively.

These results are in agreement with the aforementioned depth-related variation of the charge distribution within the 2:1 layer of smectite estimated from Li-saturated samples. Furthermore, they indicate a slightly wider range of variation of both tetrahedral and octahedral charge distribution. Indeed, the percentage of tetrahedral charge increases from 6 to 100% with increasing depth, suggesting a depth-related transition from nearly pure montmorillonite to pure beidellite in the geothermal field.

### Oxygen isotope variation

**Smectite.** Analyses of oxygen isotopes were performed on 10 samples of smectites of the geothermal field: 6 samples collected in the boreholes and 4 surface samples. Both the octahedral charge and the  $\delta^{18}O$  values obtained for these 10 smectites are given in Table 6. The  $\delta^{18}O$  values of smectites and percentage of octahedral charge collected in boreholes decrease with increasing depth (or temperature) from 15.9 to 9.8‰ (67–163 °C) and from 78 to 18% (FTIR data), respectively. The  $\delta^{18}O$  values and the percentages of octahedral charge of the surface smectite col-

TABLE 5.—EXTENDED

BO6-160 17		BO7-190 18		BO7-229 36		BO6-230 7		BO6-236 8		BO6-260 18	
av.	st. dev	av.	st. dev	av.	st. dev	av.	st. dev	av.	st. dev	av.	st. dev
3.49	0.04	3.66	0.04	3.60	0.03	3.55	0.02	3.61	0.03	3.53	0.02
0.51	0.04	0.34	0.04	0.40	0.03	0.45	0.02	0.39	0.03	0.47	0.02
1.87	0.02	1.92	0.03	1.91	0.03	1.89	0.07	1.93	0.02	1.94	0.04
0.08	0.02	0.04	0.01	0.07	0.02	0.03	0.02	0.04	0.01	0.02	0.02
0.07	0.01	0.05	0.02	0.03	0.01	0.04	0.04	0.04	0.02	0.04	0.01
0.00	0.00	0.00	0.01	0.00	0.00	0.04	0.04	0.01	0.01	0.01	0.02
0.00	0.00	0.00	0.00	0.00	0.00	0.01	0.01	0.00	0.00	0.00	0.00
2.02	0.02	2.01	0.02	2.01	0.02	2.01	0.03	2.02	0.01	2.01	0.01
0.16	0.02	0.15	0.04	0.17	0.03	0.16	0.02	0.11	0.03	0.19	0.02
0.05	0.02	0.04	0.02	0.06	0.01	0.06	0.03	0.12	0.03	0.05	0.03
0.14	0.02	0.05	0.02	0.06	0.02	0.05	0.01	0.02	0.02	0.03	0.02
0.52	0.05	0.39	0.09	0.46	0.07	0.44	0.08	0.36	0.05	0.45	0.03
2	6	13	9	13	5	0	4	0	3	0	3
98	6	87	9	87	5	100	4	100	3	100	3

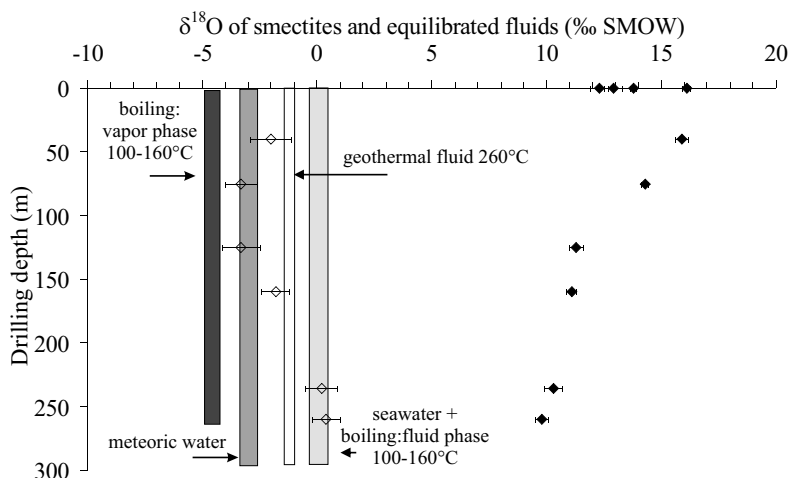


FIGURE 9. Variation of  $\delta^{18}\text{O}$  values of smectites (solid diamonds) and  $\delta^{18}\text{O}$  of fluids equilibrated with smectites calculated using the fractionation equation of Savin and Gilg (1996) (open diamonds).  $\delta^{18}\text{O}$  values of meteoric water, of geothermal fluids, and of residual fluids and vapor after boiling of the geothermal fluid are reported. The isotopic fractionation between the vapor and liquid phases is deduced from Henley et al. (1984) and Arnason (1977).

lected in a mud pool and in steaming ground range from 13.8 to 16.1‰ and from 72 to 79%, respectively. The  $\delta^{18}\text{O}$  values and the percentage of octahedral charge of the fracture-sealing smectite collected in fossil parts of the surficial geothermal field range from 12.3 to 12.9‰ and from 27 to 34%, respectively.

Using the present-day temperature, the  $\delta^{18}\text{O}$  values of the fluids in equilibrium with the smectites collected in the boreholes were calculated from Equation 1 (Sheppard and Gilg 1996). In the absence of temperature data, the  $\delta^{18}\text{O}$  values of fluid equilibrated with the surficial smectites were not estimated.

The calculated  $\delta^{18}\text{O}_{\text{fluid}}$  values range from 0.4 to -3.3‰ and their plots extend from that of the meteoric waters of the area ( $\delta^{18}\text{O} = -3.0 \pm 0.5\text{‰}$ ) to values slightly heavier than those of the fluids from the geothermal reservoir ( $\delta^{18}\text{O} = -1.1 \pm 0.2\text{‰}$  at 260 °C; Sanjuan et al. 2001). Such heavier values could correspond to residual fluids after boiling of the geothermal fluid during its

ascension and cooling down to 100 °C. Indeed, the  $\delta^{18}\text{O}$  values measured for the liquid and vapor phases of the geothermal fluid obtained after separation at 160 °C and 7 bar are  $-0.4 \pm 0.2\text{‰}$  and  $-3.9 \pm 0.2\text{‰}$ , respectively. The values measured after phase separation in the weir box at 100 °C and 1 bar are  $0.4 \pm 0.2\text{‰}$  for the separated brine and  $-5.0 \pm 0.2\text{‰}$  for the vapor. These values are very close to those estimated following the equation proposed by Arnason (1977), which gives values of  $-0.3\text{‰}$  for the liquid phase and  $-4.2\text{‰}$  for the vapor phase after phase separation at 160 °C and values of  $0.4\text{‰}$  for the liquid phase and  $-4.9\text{‰}$  for the vapor phase after phase separation at 100 °C and 1 bar (Fig. 9). These values are also close to those estimated following the equation proposed by Henley et al. (1984), which gives  $\delta^{18}\text{O}$  values of  $0.5 \pm 0.3\text{‰}$  for the separated brine and  $-4.4 \pm 0.5\text{‰}$  for the separated vapor at 100 °C.

From 40 to 150 m, the  $\delta^{18}\text{O}$  of fluids in equilibrium with

**TABLE 6.** Oxygen isotope data of smectites and calcite

Samples	Octahedral layer charge (%) of smectite	$\delta^{18}\text{O}(\text{‰})_{\text{SMOW}}$ smectite	$\delta^{18}\text{O}(\text{‰})_{\text{SMOW}}$ fluid (s)	$\delta^{18}\text{O}(\text{‰})_{\text{SMOW}}$ calcite	$\delta^{18}\text{O}(\text{‰})_{\text{SMOW}}$ fluid (c)
Surficial sampling					
S1	72	$13.8 \pm 0.1$	–	–	–
S2	79	$16.1 \pm 0.1$	–	–	–
S3	34	$12.3 \pm 0.4$	–	–	–
S4	27	$12.9 \pm 0.4$	–	–	–
Drill hole sampling					
BO7 40 m	78	$15.9 \pm 0.3$	$-2.1 \pm 0.9$	17.9	$-3.1 \pm 0.7$
BO6 75 m	64	$14.3 \pm 0.1$	$-2.6 \pm 0.7$	16.4	$-4.4 \pm 0.8$
BO6 125 m	43	$11.3 \pm 0.3$	$-3.3 \pm 0.8$	10.1	$-7.3 \pm 0.6$
BO6 160 m	2	$11.1 \pm 0.2$	$-1.8 \pm 0.6$	7.8	$-7.8 \pm 0.5$
BO6 236 m	21	$10.3 \pm 0.4$	$0.2 \pm 0.7$	7.2	$-5.3 \pm 0.4$
BO6 260 m	18	$9.8 \pm 0.3$	$0.4 \pm 0.6$	7.9	$-3.8 \pm 0.4$

Notes: The  $\delta^{18}\text{O}_{\text{SMOW}}$  values of fluids equilibrated with smectites (s) and calcite (c) were calculated using the fractionation equation of Savin and Gilg (1996) and Friedman and O'Neil et al. (1977), respectively.

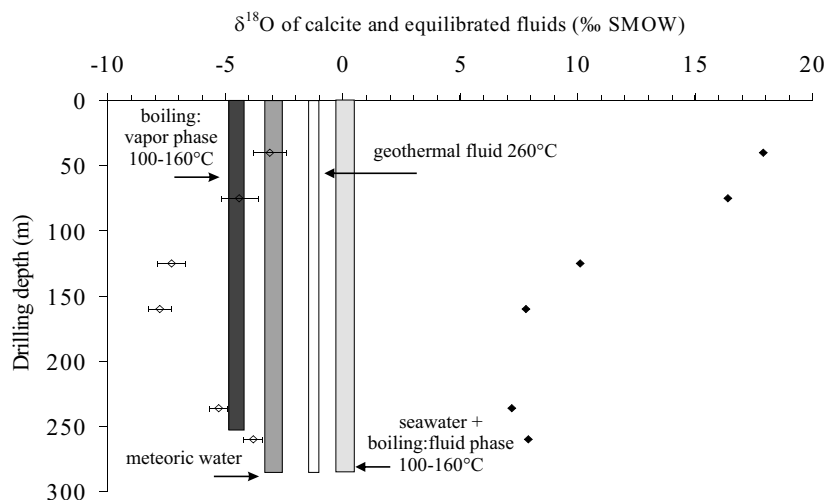


**FIGURE 10.** Variation of  $\delta^{18}\text{O}$  values of calcite (solid diamonds) and  $\delta^{18}\text{O}$  of fluids equilibrated with calcite calculated using the fractionation equation of O'Neil et al. (1969) (open diamonds).  $\delta^{18}\text{O}$  values of meteoric water, of geothermal fluids, and of residual fluids and vapor after boiling of the geothermal fluid are reported. The isotopic fractionation between the vapor and liquid phases is deduced from Henley et al. (1984) and Arnason (1977).

smectites at the given temperatures seems strongly influenced by meteoric waters and/or possibly liquids resulting from condensed vapors. Deeper than 150 m, the  $\delta^{18}\text{O}$  of fluids is strongly shifted toward those of the geothermal fluids and/or the residual fluids of their boiling. The intermediate  $\delta^{18}\text{O}_{\text{fluid}}$  values shown in Figure 9 indicate mixing of the aforementioned types of fluids. However, limited contribution of seawater cannot be excluded for surface and shallow samples.

**Calcite.** Analyses of oxygen isotopes were performed on the borehole samples previously selected for smectite analyses. The  $\delta^{18}\text{O}$  values of calcite range from 17.9 to 7.9‰ and decrease with increasing depth (or temperature) (Fig. 10). Assuming that calcite was isotopically equilibrated with fluids at the present-day temperature, the calculated  $\delta^{18}\text{O}$  values display the same trend with depth (and temperature) as those deduced from smectite analyses but are shifted to a lighter range, from  $-3.1$  to  $-7.8$ ‰ (Fig. 10). These plots extend from values slightly lower than those of the condensed vapors deduced by Henley et al. (1984) to values close to those of meteoric water. These values also support the existence of different types of fluids and the occurrence of deeper boiling processes. The lowest values of  $\delta^{18}\text{O}_{\text{fluid}}$  can be explained by the occurrence in the samples of small amounts of calcite of

propylitic origin crystallized at higher temperatures (as evidenced by their association with some relicts of chlorite).

## DISCUSSION

In this study it has been shown that the dioctahedral smectites formed within the uppermost alteration zone of the active geothermal field of Bouillante are low-charge smectites with a wide range of variation in their crystal structure and charge location. The expansion behavior and the FTIR characteristics obtained when the treatment for the Greene-Kelly test was carried out on the samples (Table 4) and the structural formulae calculated from microprobe analyses (Fig. 11) demonstrate an apparent transition from montmorillonite [ $\text{Si}_4\text{Al}_{2-x}\text{R}_x^2+\text{M}_x^+\text{O}_{10}(\text{OH})_2$ ] to beidellite [ $\text{Si}_{4-x}\text{Al}_x\text{Al}_2\text{M}_x^+\text{O}_{10}(\text{OH})_2$ ] with increasing depth (40–260 m) and temperature (67–163 °C). This mineralogical transition proceeded through interstratification of beidellite-like layers with montmorillonite-like layers and is marked by an increasing homogeneity of the layer charge of the smectite.

Montmorillonite (in the broad sense, i.e., tetrahedral charge < octahedral charges) predominates at temperatures lower than 100 °C, whereas beidellite predominates between 110 and 163 °C.

The depth-related transition from montmorillonite to beidel-

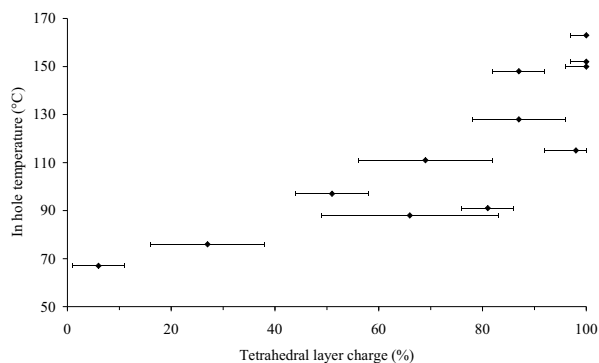


FIGURE 11. Variation of the smectite tetrahedral layer charge as a function of the present-day temperature.

lite already has been reported in several subsurface geological systems affected by high thermal gradients. In active geothermal systems, Al-rich smectites precipitated from the geothermal solutions at temperatures up to 150 °C (Inoue et al. 2004). In the active geothermal field of Chipilapa (Papapanagiotou et al. 1993; Papapanagiotou 1994), montmorillonite has been identified as the dominant type of smectite within the upper part of the alteration sequence ( $T < 130$  °C), whereas pure beidellite has been identified deeper, at higher temperature (up to 200 °C). Inoue et al. (2004) and Yang et al. (2001) described a similar depth-related montmorillonite to beidellite transition in the active geothermal systems of Kakkonda and Broadlands-Ohaaki, respectively.

A depth-related montmorillonite to beidellite transition has been also documented in tertiary sandstones and shales in Niigata (Japan) by Sato et al. (1996). In such a diagenetic environment, the vertical montmorillonite to beidellite transition is considered as the first step of the “so-called” smectite to illite reaction. Montmorillonite is progressively converted to beidellite with increasing temperature and beidellitization proceeds via a continuous solid-state Al-for-Si substitution mechanism.

In spite of the very distinct crystallization process of Al-rich smectites in geothermal and diagenetic systems (precipitation vs. solid-state transformation), a thermal control of the observed montmorillonite to beidellite transition has been invoked by all the authors. Such thermal control is supported by these data and previous studies that demonstrated that beidellite is stable at higher temperatures than montmorillonite and/or montmorillonite-beidellite mixed-layer minerals (Yamada et al. 1991; Yamada and Nakazawa 1993) and that montmorillonite can be experimentally converted to beidellite + minor amounts of Mg-rich trioctahedral smectite (stevensite or saponite) at relatively low temperatures ranging between 100 and 200 °C (Beaufort et al. 2001).

However, even if the total amount of montmorillonite-like layers is at a maximum in the shallowest samples of smectite and, conversely, the total amount of beidellite-like layers is at a maximum in the deepest samples of smectite, the vertical transition from montmorillonite to beidellite observed in the geothermal field of Bouillante is irregular. It is not strictly correlated to the present temperatures, and saponite has never been characterized in the presence of beidellite. This fact has been

verified both in the samples from the wells (Fig. 11) and from the surface. Moreover, the irregular aspect of the depth-related montmorillonite to beidellite transition cannot be explained by variations of bulk-rock chemistry because the chemical composition of the altered rocks (mostly composed of tuffs and lahars) does not vary significantly over the thickness of the uppermost alteration zone (Guisseau 2005).

The above considerations lead us to propose that the transition montmorillonite-beidellite observed at Bouillante is not due to a thermally controlled beidellitization process as defined by Sato et al. (1996), but that it is related to the hydrothermal solutions from which precipitated the Al-rich smectites precipitated. The validation of this hypothesis can be addressed through the interpretation of the oxygen isotope data of smectites and associated calcite acquired in this study. Those data indicate that the changes in oxygen-isotopic composition of the smectites cannot be explained by the temperature variation of a fluid having a unique origin (Fig. 9). In the geothermal field of Bouillante, the depth-related variation of the oxygen isotope composition of the dioctahedral smectites can be explained much more satisfactorily using different origins of the solutions involved in the mineralogical reactions. Five distinct fluid sources can be invoked to explain the  $\delta^{18}\text{O}$  values of fluids equilibrated with the smectites at the present temperatures: (1) geothermal fluid from deep reservoirs; (2) residual solutions from boiling of the geothermal fluid; (3) fluids resulting of the condensation of vapors extracted from the boiling zones; (4) meteoric waters of the free water table; and (5) a limited seawater contribution(?). However, the latter contribution appears unrealistic to explain the  $\delta^{18}\text{O}$  of smectites crystallized in depth considering their aluminous chemical composition.

The  $\delta^{18}\text{O}$  values calculated for the fluids equilibrated with the smectites indicate that beidellite-rich smectite precipitated from reacting solutions whose origin has to be sought essentially in the hot geothermal fluid from the deep geothermal reservoir associated with minor amounts of residual solutions resulting from local boiling (as supported petrographically by the local occurrence of bladed calcite). In the same way, montmorillonite-rich smectite precipitated from reacting solutions whose origin has to be searched in the phreatic water table of the Bouillante area associated with minor amounts of liquids resulting from the condensation of vapors that escaped from the deeper boiling zones (as supported by oxygen isotopic compositions of calcite). The irregular depth-related variations of both the oxygen isotope composition and the crystal-chemical properties of the smectites characterized in this study could be indicative of a local change in the respective proportion of the distinctive source fluids involved in the mineral reactions.

The above interpretation is confirmed by the variation in the Mg content of the smectites. The very low amounts of Mg measured in the waters collected in the wells, less than 10 mg/L, (Brombach et al. 2000; Traineau et al. 1997; Sanjuan et al. 2001) preclude a direct precipitation of Mg-bearing smectite from such hydrothermal solution. Conversely, in absence of sea water, Mg enrichment of the surficial springs (Brombach et al. 2000) is an expected consequence of the weathering processes that tend to leach Mg from the altered andesitic rocks. Indeed, as generally observed in the volcanic islands of the Lesser Antilles (Robert

and Herbillon 1992), weathering of the andesitic volcanic rocks that crop out at Bouillante under tropical conditions (Patrier et al. 2003) promoted the formation of Mg-free clay minerals (halloysite, kaolinite, and kaolinite-smectite mixed layers). The broad positive correlation between Mg content and  $\delta^{18}\text{O}$  values of the smectites from the geothermal field of Bouillante (Fig. 12) confirms that the mixing rate of Mg-free geothermal fluid from the deep reservoir with surficial waters from the free water table can exert a major influence on the montmorillonite vs. beidellite ratio of the smectite material. The deviations from this general trend, which have been observed locally (at a depth of 125 m for instance), could be indicative of a significant contribution of fluids derived from boiling process (Mas et al. 2006).

### CONCLUDING REMARKS

In this study, it has been demonstrated that the depth-related montmorillonite to beidellite transition documented in the uppermost alteration zone of the active geothermal field of Bouillante results from a dual control imposed on the one hand by the high geothermal gradient existing at present, and on the other hand, by the chemical nature of the solutions involved in the mineralogical reactions. Temperature and fluid chemistry are not independent factors in the fracture-controlled hydrothermal systems (Bignall and Browne 1994; Inoue et al. 1999, 2004; Liakopoulos et al. 1991; Ramos 2002; Teklemariam et al. 1996; Utami 2000) in which most of the heat transfer is supplied by convective and/or advective fluid flow between both the recharge and discharge zones. This led us to regard the crystal-chemical variations of dioctahedral smectites documented in the uppermost alteration zone of the geothermal field of Bouillante as a marker of the hydrological structure of the geothermal field. Beidellite crystallizes from Mg-free hot fluids ascending from deeper levels in discharge zones in which fluid temperature can locally exceed the water boiling curve as indicated by shallow boiling and hot springs, whereas the crystallization of montmorillonite is triggered by downward infiltration of cold surficial and mainly meteoric waters in recharge zones ( $\pm$ condensation of vapors escaping from deeper boiling zones). The heterogeneous mixing of these different types of fluids reflected in the irregular depth-related montmorillonite-beidellite transition observed in the wells would result from the complexity of their circulation path within the outermost alteration zone. In the same way, both

the crystal-chemical and the oxygen-isotope compositions of the smectites collected in the fossil hydrothermal veins identified at the surface of the geothermal field in areas where no hydrothermal activity still persists are indicative of a past discharge along fractures of hot fluids similar to those presently ascending in the active hydrothermal areas.

In conclusion, this study enhances the relevance of determining the crystal-chemical properties of dioctahedral smectites in both the active and fossil geothermal fields related to intra-oceanic subduction systems such as the Lesser Antilles island arc. In these geothermal systems, precipitation of beidellite from near-neutral fluids is strictly related to deeper high-temperature geothermal activity. Indeed, the isotopic composition of the fluids in equilibrium with the dioctahedral smectites reveals that beidellite-rich smectites are in equilibrium with high-temperature fluids that issued from geothermal reservoirs, whereas the montmorillonite-rich smectites formed from downward infiltration of the surficial waters. As a consequence, the occurrence of beidellite at or near the surface of the geothermal fields can then be used as a prospecting guide for hidden high-enthalpy geothermal reservoirs of economic interest.

### ACKNOWLEDGMENTS

Financial support for this study was provided by ADEME and the Research Division of BRGM. The authors are grateful to the staff of GEOTHERMIE BOUILLANTE, CFG Services for site facilities.

### REFERENCES CITED

- Arnason, B. (1977) The hydrogen-water isotope thermometer applied to geothermal areas in Iceland. *Geothermics*, 5, 75–80.
- Bargar, K.E. and Beeson, M.H. (1981) Hydrothermal alteration in research drill hole Y-2, Lower Geysir Basin, Yellowstone National Park, Wyoming. *American Mineralogist*, 66, 473–490.
- Battaglia, S. (2004) Variations in the chemical composition of illite from five geothermal fields: A possible geothermometer. *Clay Minerals*, 39, 501–510.
- Beaufort, D., Papapanagiotou, P., Patrier, P., Fouillac, A.M., and Traineau, H. (1996) I/S and C/S mixed layers, some indicators of recent physical-chemical changes in active geothermal systems: The case study of Chipilapa (El Salvador). Proceedings of the 21<sup>th</sup> Workshop on Geothermal Reservoir Engineering, Stanford, California.
- Beaufort, D., Berger, G., Lachapagne, J.C., and Meunier, A. (2001) An experimental alteration of montmorillonite to a di + trioctahedral smectite assemblage at 100 and 200 °C. *Clay Minerals*, 36, 211–225.
- Bignall, G. and Browne, P.R.L. (1994) Surface hydrothermal alteration and evolution of the Te Kopia thermal area, New Zealand. *Geothermics*, 23, 5/6, 645–658.
- Bish, D.L. and Reynolds, Jr., R.C. (1989) Sample preparation for X-ray diffraction. In D.L. Bish and J.E. Post, Eds., *Modern Powder Diffraction*, 20, p. 73–99. Reviews in Mineralogy, Mineralogical Society of America, Chantilly, Virginia.
- Brombach, T., Marini, L., and Hunziker, J.C. (2000) Geochemistry of the thermal springs and fumaroles of Basse-Terre Island, Guadeloupe, Lesser Antilles. *Bulletin of Volcanology*, 61, 477–490.
- Browne, P.R.L. and Ellis, A.J. (1970) The Ohaaki-Broadlands hydrothermal area, New-Zealand. *Mineralogy and related geochemistry. American Journal of Science*, 269, 97–131.
- Calvet, R. and Prost, R. (1971) Cation migration into empty octahedral sites and surface properties of clays. *Clays and Clay Minerals*, 19, 175–186.
- Cathelineau, M., Oliver, R., Nieva, D., and Garfias, A. (1985) Mineralogy and distribution of hydrothermal mineral zones in Los Azufres (Mexico) geothermal field. *Geothermics*, 1, 49–57.
- Clayton, R.N. and Mayeda, T.K. (1963) The use of bromine pentafluoride in the extraction of oxygen from oxides and silicates for isotope analysis. *Geochimica et Cosmochimica Acta*, 27, 43–52.
- Cole, D.R. and Ravinsky, L.I. (1984) Hydrothermal alteration zoning in the Beowave geothermal system, Eureka and Lander counties, Nevada. *Economic Geology*, 79, 759–767.
- Drits, V.A., Salyn, A.L., and Sucha, V. (1996) Structural transformations of interstratified illite-smectite from Dolna Ves hydrothermal deposits: dynamics and mechanisms. *Clays and Clay Minerals*, 44, 191–190.
- Farmer, V.C. (1974) *The Infrared Spectra of Minerals*, p. 331–365 (The layers silicates). Mineralogical Society (Monograph), London.

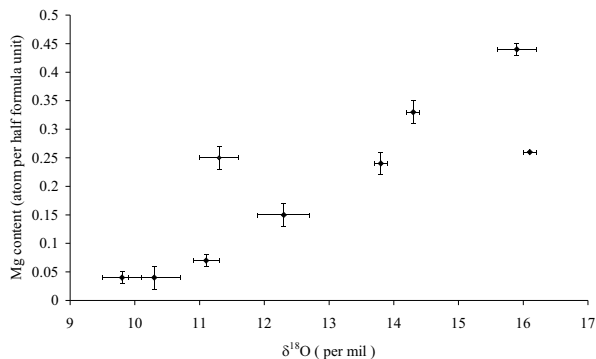


FIGURE 12. Variation of the Mg content of smectite as a function of their  $\delta^{18}\text{O}$  values.

- Feuillet, N., Manighetti, I., Taponnier, P., and Jacques, E. (2002) Arc parallel extension and localization of volcanic complexes in Guadeloupe, Lesser Antilles. *Journal of Geophysical Research*, 107, B12(2), 1–28.
- Flexser, S. (1991) Hydrothermal alteration and past and present thermal regimes in the western moat of Long Valley caldera. *Journal of Volcanology and Geothermal Research*, 48, 303–318.
- Friedman, I. and O'Neil, J.R. (1977) Compilation of stable isotope fractionation factors of geochemical interest. In M. Fleisher, Ed., *Data of geochemistry*, 12 p. U.S. Geological Survey Professional Paper 440-KK, 6th ed., Reston, Virginia.
- Girard, J.P., Razanadradosoa, D., and Freyssinet, P. (1997) Laser oxygen isotope analysis of weathering goethite from the lateritic profile of Yaou, French Guiana: Paleoweathering and paleoclimatic implications. *Applied Geochemistry*, 12, 163–174.
- Greene-Kelly, R. (1953) Irreversible dehydration in montmorillonite. Part II. *Clay Mineral Bulletin*, 2, 52–56.
- Guisseau, D. (2005) Signature des conditions dynamiques (thermiques, hydrodynamiques...) dans les propriétés des argiles du champ géothermique de Bouillante—Guadeloupe, 194 p. Ph.D. thesis, University of Poitiers, France.
- Güven, N. (1988) Smectites. In S.W. Bailey, Ed., *Hydrous Phyllosilicates*, 19, p. 497–559. *Reviews in Mineralogy*, Mineralogical Society of America, Chantilly, Virginia.
- Harvey, C.C. and Browne, P.R.L. (1991) Mixed-layer clay geothermometry in the Wairakei geothermal field, New Zealand. *Clays and Clay Minerals*, 39(6), 614–621.
- Henley, R.W., Truesdell, A.H., Barton, Jr., P.B., and Whitney, J.A. (1984) Fluid-mineral equilibria in hydrothermal systems. In J.M. Robertson, Ed., *Reviews in Economic Geology*, 1, p. 129–142 (Chapter 10). *Society of Economic Geologists*, El Paso, Texas.
- Hoffman, U. and Klemen, R. (1950) Verlust der austauschfähigkeit von lithiumionen an bentonite durch. *Zeitschrift für Anorganische und Allgemeine Chemie*, 262, 95–99.
- Hulen, J.B. and Nielson, D.L. (1984) Hydrothermal alteration in the Baca geothermal system, Redondo dome, Valles caldera, New Mexico. *Journal of Geophysical Research*, 91(B2), 1867–1886.
- Inoue, A. (1995) Formation of clay minerals in hydrothermal environments. In B. Velde, Ed., *Origin and Mineralogy of Clays*, p. 268–329. Springer-Verlag, Berlin.
- Inoue, A. and Kitagawa, R. (1994) Morphological characteristics of illite clay minerals from a hydrothermal system. *American Mineralogist*, 79, 700–711.
- Inoue, A., Velde, B., Meunier, A., and Touchard, G. (1988) Mechanism of smectite-to-illite conversion in a hydrothermal system. *American Mineralogist*, 73, 1325–1334.
- Inoue, A., Utada, M., and Shimizu, M. (1999) Mineral-fluid interactions in the Sumikawa geothermal system, Northeast Japan. *Resource Geology Special Issue*, 20, 79–98.
- Inoue, A., Meunier, A., and Beaufort, D. (2004) Illite-smectite mixed layer minerals during in felsic volcanoclastic rocks from drill cores, Kakkonda, Japan. *Clay and Clay Minerals*, 52, 66–84.
- Ji, J. and Browne, P.R.L. (2000) Relationship between illite crystallinity and temperature in active geothermal systems of New Zealand. *Clays and Clay Minerals*, 48, 139–144.
- Lanson, B. and Besson, G. (1992) Characterization of the end of smectite-to-illite transformation: Decomposition of X-ray patterns. *Clays and Clay Minerals*, 40, 40–52.
- Liakopoulos, A., Katerinopoulos, A., Markopoulos, T., and Boulegue, J. (1991) A mineralogical petrographic and geochemical study of samples from wells in the geothermal field of Milos island (Greece). *Geothermics*, 20(4), 237–256.
- Lowell, J.D. and Guilbert, J.M. (1970) Lateral and vertical alteration and mineralization zoning in porphyry ore deposits. *Economic Geology*, 65, 373–408.
- MacEwan, D.M.C. and Wilson, M.J. (1980) Interlayer and intercalation complexes of clay minerals. In G.W. Brindley and G. Brown, Eds., *Crystal Structures of Clay Minerals and their X-ray Identification*, p. 197–248. Mineralogical Society, London.
- Malfoy, C., Pantet, A., Monnet, P., and Righi, D. (2003) Effects of the nature of the exchangeable cation and clay concentration on the rheological properties of smectite suspensions. *Clays and Clay Minerals*, 51, 656–663.
- Mas, A., Guisseau, D., Patrier, P., Beaufort, D., Genter, A., Girard, J.P., and Sanjuan, B. (2006) Clay minerals related to the hydrothermal activity of the Bouillante geothermal field (Guadeloupe). *Journal of Volcanology and Geothermal Research*, 158, 380–400.
- McCrea, J.M. (1950) On the isotopic composition chemistry of carbonate and paleotemperature scale. *Journal of Chemistry and Physics*, 18, 849–857.
- Moore, D.M. and Reynolds, Jr., R.C. (1997) X-Ray diffraction and the identification and analysis of clay minerals, 2<sup>nd</sup> ed., 378 p. Oxford University Press, U.K.
- Olis, A.C., Malla, P.B., and Douglas, L.A. (1990) The rapid estimation of the layer charges of 2:1 expanding clays from a single alkylammonium ion expansion. *Clay Minerals*, 25, 39–50.
- O'Neil, J.R., Clayton, R.N., and Mayeda, T.K. (1969) Oxygen isotope fractionation in divalent metal carbonates. *Journal of Chemistry and Physics*, 51, 5547–5558.
- Papapanagiotou, P. (1994) Evolution des minéraux argileux en relation avec la dynamique des champs géothermiques de haute enthalpie: l'exemple du champ de Chipilapa (Salvador), 189 p. Ph.D. thesis, University of Poitiers, France.
- Papapanagiotou, P., Beaufort, D., Patrier, P., and Traineau, H. (1993) Clay mineralogy of the >0.2 µm rock fraction of the M1 drill hole of the geothermal field of Milos (Greece). *Bulletin of the Geological Society of Greece*, 28, 575–586.
- Patrier, P., Beaufort, D., Mas, A., and Traineau, H. (2003) Surficial clay assemblage associated with the hydrothermal activity of Bouillante (Guadeloupe, FWI). *Journal of Volcanology and Geothermal Research*, 126, 143–156.
- Petit, S., Righi, D., Madejova, J., and Decarreau, A. (1998) Layer charge estimation of smectites using infrared spectroscopy. *Clay Minerals*, 33, 579–591.
- Ramos, S.G. (2002) Potential constraints to the development of the Rangas sector based on petrologic evaluation of the Bacman geothermal field, Philippines. *Proceedings, 27<sup>th</sup> Workshop on Geothermal Reservoir Engineering*, Stanford, California, January 28–30, 2002, SGP-TR-171.
- Reyes, A.G. (1990) Petrology of Philippine geothermal systems and the application of alteration mineralogy to their assessment. *Journal of Volcanology and Geothermal Research*, 43, 279–309.
- Reynolds, R.C. (1985) Description of program NEWMOD for the calculation of the one-dimensional X-ray diffraction patterns of mixed-layered clays, 23 p. Department of Earth Sciences, Dartmouth College, Hanover, New Hampshire.
- Righi, D. and Meunier, A. (1995) Origin of clays by rock weathering and soil formation. In B. Velde, Ed., *Origin and Mineralogy of Clays*, p. 43–161. Springer, Berlin.
- Righi, D., Petit, P., and Bouchet, A. (1993) Characterization of hydroxy-interlayered vermiculite and illite/smectite interstratified minerals from the weathering of chlorite in cryorhod. *Clays and Clay Minerals*, 41, 484–495.
- Robert, M. and Herbillon, A. (1992) Application aux argiles des sols. Genèse, nature et rôle des constituants argileux dans les principaux types de sols des environnements volcaniques insulaires. *Matériaux argileux: Structure, Propriétés et Applications*. SFMC-GFA, Chapter 3, p. 540–576.
- Russel, J.D. and Fraser, A.R. (1994) Infrared methods. In M.J. Wilson, Ed., *Clay mineralogy: Spectroscopic and chemical determinative methods*, p. 11–67. Chapman and Hall, London.
- Sanjuan, B., Lasne, E., and Brach, M. (2000) Bouillante geothermal field (Guadeloupe, West Indies): Geochemical monitoring during a thermal stimulation operation. *Proceedings of the 25<sup>th</sup> Workshop on Geothermal Reservoir Engineering*, Stanford.
- Sanjuan, B., Brach, M., and Lasne, E. (2001) Bouillante geothermal fluid: mixing and water/rock interaction processes at 250 °C. In R. Cidu, Ed., *Proceedings of the 10<sup>th</sup> international symposium on water/rock interactions (WRI 10)*, 10–15 July 2001, vol. 2, p. 911–914. A.A. Balkema publishers, Villasimius (Italy).
- Sato, T., Murakami, T., and Watanabe, T. (1996) Change in layer charge of smectites and smectite layers in illite/smectite during diagenetic alteration. *Clays and Clay Minerals*, 44, 460–469.
- Seki, Y. (2000) Hydrothermal alteration in the Sunagohara formation, Okuazu geothermal system, Japan. *Proceedings World Geothermal Congress, Kyushu-Tohoku, Japan, May 28–June 10, 2000*, p. 1719–1724.
- Sheppard, S.M.F. and Gilg, H.A. (1996) Stable isotope geochemistry of clays. *Clay Minerals*, 31, 1–24.
- Teklemariam, M., Battaglia, S., Gianelli, G., and Ruggieri, G. (1996) Hydrothermal alteration in the Aluto-Langano geothermal field, Ethiopia. *Geothermics*, 25(6), 679–702.
- Traineau, H., Sanjuan, B., Beaufort, D., Brach, M., Castaing, C., Correia, H., Genter, A., and Herbrich, B. (1997) The Bouillante geothermal field (F.W.I.) revisited: New data on the fractured geothermal reservoir in light of a future simulation experiment in a low productive well. *Proceedings of the 22<sup>nd</sup> Workshop on Geothermal Reservoir Engineering*, Stanford, 1997, p. 97–103.
- Utami, P. (2000) Characteristics of the Kamojang geothermal reservoir (West Java) as revealed by its hydrothermal alteration mineralogy. *Proceedings World Geothermal Congress 2000, Kyushu-Tohoku, Japan, May 28–June 10, 2000*.
- Velde, B. (1985) Clay minerals: A physico-chemical explanation of their occurrence, 40, 427 p. *Developments in Sedimentology*, Elsevier, Amsterdam.
- (1986) Compositional variation in component layers in natural illite/smectites. *Clays and Clay Minerals*, 34(6), 651–657.
- Wohletz, K. and Heiken, G. (1992) *Volcanology and geothermal energy*, Chapter 3, p. 119–140. University of California Press, Berkeley.
- Yamada, H. and Nakazawa, H. (1993) Isothermal treatments of regularly interstratified montmorillonite-beidellite at hydrothermal conditions. *Clays and Clay Minerals*, 41, 726–730.
- Yamada, H., Nakazawa, H., Yoshioka, K., and Fujita, T. (1991) Smectites in the montmorillonite-beidellite series. *Clay Minerals*, 26, 359–369.
- Yang, K., Browne, P.R.L., Huntington, J.F., and Walshe, J.L. (2001) Characterising the hydrothermal alteration of the Broadlands-Ohaaki geothermal system, New Zealand, using short-wave infrared spectroscopy. *Journal of Volcanology and Geothermal Research*, 106, 53–65.

MANUSCRIPT RECEIVED JULY 27, 2006

MANUSCRIPT ACCEPTED JULY 20, 2007

MANUSCRIPT HANDLED BY ROBERT DYMEK